arXiv:cond-mat/9802006v1 [cond-mat.supr-con] 1 Feb 1998

Temperature Dependence of Even-Odd Effects in Small Superconducting Systems

R. Balian[1], H. Flocard[2], and M. Véneroni[2]
[1] *S.Ph.T, CEA, Saclay, F-91191, Gif sur Yvette Cedex*
[2] *Division de Physique Théorique, Institut de Physique Nucléaire, F-91406 , Orsay Cedex*
(January 1998)

Generalized BCS equations which consistently include the projection on the particle-number parity are derived from a systematic variational method. Numerical solutions are given that are illustrative of ultra-small metallic grains. Compared to the BCS approximation, the pairing is slightly enhanced in even and noticeably inhibited in odd systems. In the latter case, the gap increases with T near $T = 0$; for a suitably small pairing this can result in a reentrance phenomenon. Paramagnetic effects are evaluated as functions of the temperature and the magnetic field.

PACS numbers: 21.60.-n, 74.20.Fg, 74.25.Bt, 74.80.Fp

The qualitative differences between the properties of even and odd nuclei have long been known, as well as their explanation by pairing correlations [1]. Even-odd effects have also been displayed in recent years in superconducting metallic islands [2] and, during the last two years, in ultra-small Aluminium grains [3]. In the nuclear case, the ground and lowest excited states are successfully described by the BCS theory and its Hartree-Fock-Bogoliubov (HFB) generalization [4]. Indeed, at zero temperature, the BCS state is a superposition of configurations with even particle number only, which allows the currently used models to discriminate between odd and even systems. However, in the case of hot nuclei (which will be investigated intensively by means of the next generation of γ-detector arrays) or of small metallic superconducting systems, the non-zero temperature BCS Ansatz mixes configurations with even and odd particle numbers that have dissimilar physical properties. This additional spurious mixing requires projecting the thermal BCS state onto subspaces having, at least, a well-defined number-parity (if not a well-defined particle number). Several theoretical studies have already been devoted to this question [5]- [8].

We rely here on a general variational scheme [9] to derive an extension of the BCS theory which consistently incorporates the number-parity (N-parity) projection. The method is devised to optimize the (unnormalized) characteristic function $\varphi(\xi) \equiv \ln \mathrm{Tr} \hat{P}_\eta \mathrm{e}^{-\beta \hat{K}} \hat{A}(\xi)$, with $\hat{K} = \hat{H} - \mu \hat{N}$ and $\hat{A}(\xi) \equiv \exp(-\sum_\gamma \xi_\gamma \hat{Q}_\gamma)$ where $\hat{H}$, $\hat{N}$, $\hat{Q}_\gamma$ and ξ_γ are the Hamiltonian, the particle-number operator, the observables of interest and the associated sources. The trace (Tr) is taken over the full Fock space. In the unnormalized equilibrium density operator $\hat{P}_\eta \mathrm{e}^{-\beta \hat{K}}$, the factor $\hat{P}_\eta$ is the projection

$$\hat{P}_\eta = \frac{1}{2}(\hat{\mathbf{1}} + \eta \mathrm{e}^{\mathrm{i}\pi \hat{N}})$$

on the subspace with even ($\eta = +1$) or odd ($\eta = -1$) particle number. To determine variationally $\varphi(\xi)$ we introduce [8] the action-like functional

$$\mathcal{I}\left\{\hat{\mathcal{D}}(\tau), \hat{\mathcal{A}}(\tau)\right\} \equiv \mathrm{Tr} \hat{\mathcal{D}}(\beta) \exp(-\sum_\gamma \xi_\gamma \hat{Q}_\gamma) - \int_0^\beta \mathrm{d}\tau \, \mathrm{Tr} \hat{\mathcal{A}}(\tau) \Big(\frac{\mathrm{d}\hat{\mathcal{D}}(\tau)}{\mathrm{d}\tau} + \frac{1}{2}[\hat{K}\hat{\mathcal{D}}(\tau) + \hat{\mathcal{D}}(\tau)\hat{K}] \Big) \, , \quad (1)$$

where the trial quantities are the operators $\hat{\mathcal{A}}(\tau)$ and $\hat{\mathcal{D}}(\tau)$. The density-like operator $\hat{\mathcal{D}}(\tau)$ is meant to include the projection factor $\hat{P}_\eta$ and to satisfy the initial boundary condition $\hat{\mathcal{D}}(0) = \hat{P}_\eta$. For unrestricted trial spaces, the stationarity conditions of the functional (1) yield the (symmetrized) Bloch equation for $\hat{\mathcal{D}}(\tau)$ and, redundantly, the Bloch analogue of the backward Heisenberg equation for $\hat{\mathcal{A}}(\tau)$ with the final boundary condition $\hat{\mathcal{A}}(\beta) = \hat{A}(\xi)$. When the trial spaces for $\hat{\mathcal{D}}(\tau)$ and $\hat{\mathcal{A}}(\tau)$ are restricted, the two equations in general become coupled and *the stationary value of the functional* (1) *provides an optimum for* $\exp \varphi(\xi)$.

We are only concerned in this letter by the evaluation of (projected) thermodynamic quantities. These are given by the limit $\xi_\gamma = 0$ (i.e., $\hat{A}(0) = \hat{\mathbf{1}}$); indeed $\varphi(0)$ is the thermodynamic potential associated with the $\hat{P}_\eta$-grand canonical equilibrium in which the particle number can fluctuate but not the N-parity. In this limit and for the trial spaces (2) that we shall use, one can check that the optimization of (1) is equivalent to the usual minimization of the thermodynamic potential [8].

For the Hamiltonian $\hat{H}$ we take, as in [7], the schematic BCS form

$$\hat{H} = \sum_p \epsilon_p (a_p^\dagger a_p + a_{\bar{p}}^\dagger a_{\bar{p}}) - B\,\hat{M} - \sum_{pq} G_{pq} a_p^\dagger a_{\bar{p}}^\dagger a_{\bar{q}} a_q \, ,$$

in which $a_p^\dagger$ and $a_{\bar{p}}^\dagger$ are the creation operators associated with the paired single-particle states p and $\bar{p}$. The magnetic-moment operator $\hat{M} \equiv \sum_p (a_{\bar{p}}^\dagger a_{\bar{p}} - a_p^\dagger a_p)$, coupled with the magnetic field B (in reduced units), gives rise to paramagnetic effects; for rotating deformed nuclei, the term $B\hat{M}$ would be replaced by $\omega \hat{J}_z$ where ω is the angular velocity and $\hat{J}_z$ the z-component of the angular momentum. The pairing coefficients G_{pq} are real, symmetric and, for simplicity, the diagonal elements G_{pp} are assumed to be zero.

As variational Ansatz we take

$$\hat{\mathcal{D}}(\tau) = \hat{P}_\eta \mathrm{e}^{-\tau \hat{W}} \ , \qquad \hat{\mathcal{A}}(\tau) = \mathrm{e}^{-(\beta-\tau)\hat{W}} \ , \qquad (2)$$

with, for the trial operator $\hat{W}$, the standard form

$$\hat{W} = h_0 - \frac{1}{2}\sum_p (e_p + e_{\bar{p}}) + \sum_p (e_p b_p^\dagger b_p + e_{\bar{p}} b_{\bar{p}}^\dagger b_{\bar{p}}) \ , \quad (3)$$

where $b_p^\dagger$ and $b_{\bar{p}}^\dagger$ are the usual quasi-particle operators ($b_p = u_p a_p + v_p a_{\bar{p}}^\dagger$, $b_{\bar{p}} = u_p a_{\bar{p}} - v_p a_p^\dagger$). In the static problem we are considering here, the quantities u_p and v_p can be taken real and non-negative, with $u_p^2 + v_p^2 = 1$. Thus our independent variational parameters are the real numbers e_p, $e_{\bar{p}}$, v_p and h_0. We get an explicit expression for the functional (1) by inserting Eqs. (2-3) and using the generalized Wick theorem [10] for the two terms generated by the projection $\hat{P}_\eta$. New projected BCS equations are obtained by writing the stationarity conditions for this expression. The familiar BCS equation for the gap is replaced by

$$\Delta_p = \frac{1}{4}\sum_q G_{pq} \frac{\Delta_q}{\tilde{e}_q}(t_q + t_{\bar{q}}) \frac{1 + \eta r_0 (t_p t_{\bar{p}} t_q t_{\bar{q}})^{-1}}{1 + \eta r_0 (t_p t_{\bar{p}})^{-1}} \quad , \quad (4)$$

where the quantities t_p, $t_{\bar{p}}$, r_0, $\tilde{e}_q$, are defined by

$$t_p \equiv \tanh(\tfrac{1}{2}\beta e_p) \ , \ t_{\bar{p}} \equiv \tanh(\tfrac{1}{2}\beta e_{\bar{p}}) \ , \ r_0 \equiv \prod_p t_p t_{\bar{p}} \ ,$$

$$\tilde{e}_p \equiv \sqrt{(\epsilon_p - \mu)^2 + {\Delta_p}^2} \quad . \qquad (5)$$

The quasi-particle energies e_p and $e_{\bar{p}}$ appearing in the thermal factors t_p and $t_{\bar{p}}$ differ from the BCS expression (5); indeed, e_p satisfies

$$e_p = \tilde{e}_p + B - \frac{\eta r_0 t_p}{{t_p}^2 - \eta r_0}\Big(\frac{x_p (t_p^{-1} + t_{\bar{p}}^{-1})}{1 + \eta r_0 (t_p t_{\bar{p}})^{-1}} + 2k_1 \Big) \ , \quad (6)$$

where x_p and k_1 are given by

$$x_p \equiv \frac{1}{4}\sum_q G_{pq} \frac{\Delta_p \Delta_q}{\tilde{e}_p \tilde{e}_q}(t_q^{-1} + t_{\bar{q}}^{-1} - t_q - t_{\bar{q}}) \quad ,$$

$$k_1 \Big[1 + \eta r_0 + \eta r_0 \sum_p \big(\frac{1 - {t_p}^2}{{t_p}^2 - \eta r_0} + p \leftrightarrow \bar{p} \big) \Big] \equiv$$
$$-\frac{1}{4}\sum_p x_p \Big[(t_p^{-1} - t_p) \frac{{t_p}^2 + \eta r_0}{{t_p}^2 - \eta r_0} + p \leftrightarrow \bar{p} \Big] \ .$$

The quasi-particle energy $e_{\bar{p}}$ is obtained from Eq.(6) by the exchanges $t_p \leftrightarrow t_{\bar{p}}$ and $B \leftrightarrow -B$. Altogether, one has to solve numerically the self-consistent Eqs. (4) and (6) for Δ_p, e_p and $e_{\bar{p}}$. The coefficients u_p and v_p are then given explicitly by the normalization condition ${u_p}^2 + {v_p}^2 = 1$ and by the relation $2u_p v_p/({u_p}^2 - {v_p}^2) = \Delta_p/(\epsilon_p - \mu)$. All the quantities Δ_p, e_p, $e_{\bar{p}}$, $\tilde{e}_p$, $r_0 = \mathrm{Tr}\ \mathrm{e}^{\mathrm{i}\pi\hat{N}}\mathrm{e}^{-\beta\hat{W}}/\mathrm{Tr}\ \mathrm{e}^{-\beta\hat{W}}$, x_p, k_1, u_p, v_p depend on the N-parity index $\eta = \pm 1$. The standard BCS equations are recovered for $\eta = 0$. In Eq. (4) the projection effects occur indirectly via e_p and $e_{\bar{p}}$, and directly through the last fraction. The form of this fraction entails : (i) a predominant influence of the states near the Fermi level, (ii) odd (even) projected gaps Δ_p smaller (larger) than their BCS counterparts, and (iii) greater deviations from BCS for the odd than for the even systems.

We further assume, as is often done, that the twofold degenerate single-particle energies ϵ_p are equally spaced with a level density w_F. We use a cut-off energy $\Lambda/2$, above and below the Fermi level, such that $w_\mathrm{F}\Lambda = 100$. The pairing coefficients G_{pq} are chosen of the form $\tilde{G}(1 - \delta_{pq})$. The projected and the BCS gaps depend on p ; however, the variations of Δ_p with p never exceed a few percent in our calculations. A convenient energy scale is provided by the BCS gap Δ associated, for $T = 0$ and $B = 0$, with the quasi-particle of lowest energy. This model, depending on the values of $w_\mathrm{F}\Delta$, or alternatively of $w_\mathrm{F}\tilde{G}$, schematically describes superconducting islands, heavy nuclei or ultra-small metallic grains. The corresponding variational equations above have been solved in Ref. [8] for $B = 0$. The results display the growing magnitude of the even-odd effects as $w_\mathrm{F}\Delta$ decreases. In view of recent experimental advances [3], we give preference here to parameters typical of ultra-small grains.

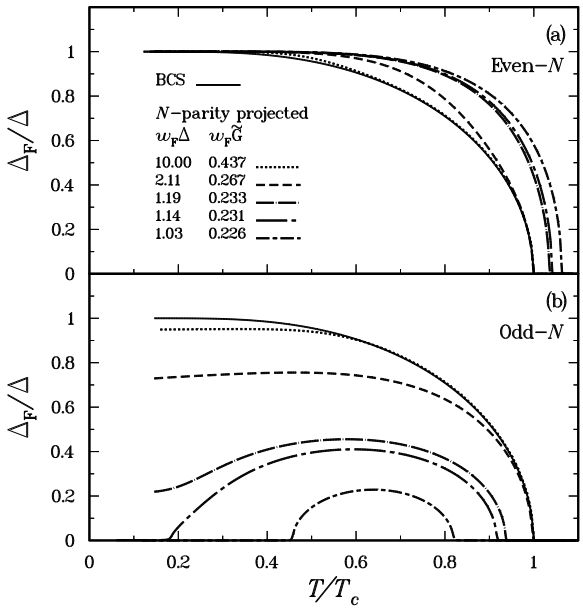


FIG. 1. Even/odd projected gaps. The gap Δ_F is plotted (for $B = 0$) as function of T for various values of $w_\mathrm{F}\Delta$, or equivalently of $w_\mathrm{F}\tilde{G}$. The upper part (a) corresponds to the even system $\langle\hat{N}\rangle = 100$ and the lower part (b) to the odd system $\langle\hat{N}\rangle = 101$.

For $B = 0$ and for various values of $w_{\rm F}\Delta$, Fig.1 shows the variation with $T/T_{\rm c}$ ($T_{\rm c}$ denotes the BCS critical temperature for $B = 0$) of the ratio $\Delta_{\rm F}/\Delta$, where $\Delta_{\rm F}$ is the temperature-dependent (odd or even) gap Δ_p associated with the quasi-particle of lowest energy e_p. According to Eq. (4), both the gap values and the critical temperatures show that pairing is enhanced (inhibited) by projection on even (odd) particle number. In the odd case, near $T = 0$, a new phenomenon appears: *the growth of the pairing correlations with temperature*. This effect can be understood as follows. At $T = 0$ the unpaired particle occupies one of the two states $\epsilon_0 = \epsilon_{\bar{0}} = \mu$, precluding them to participate to the pair components. For (small) increasing values of T, thermal excitation induces the migration of this unpaired particle to higher states, thus making the strategic states at the Fermi level available to the formation of pairs.

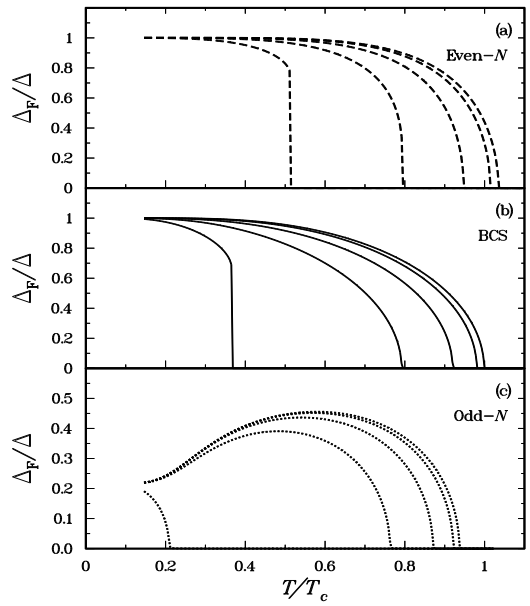


FIG. 2. Dependence upon T of the gap $\Delta_{\rm F}$ for $w_{\rm F}\Delta = 1.19$ ($w_{\rm F}\tilde{G} = 0.233$) and for magnetic-field values such that $w_{\rm F}B$=0; 0.2; 0.4; 0.6; 0.8. The three plots correspond to (a) the even-N projection ($\langle\hat{N}\rangle = 100$), (b) the BCS theory ($\langle\hat{N}\rangle = 100$), and (c) the odd-$N$ projection ($\langle\hat{N}\rangle = 101$). Note the scale difference between (c) and (a).

For suitable values of $w_{\rm F}\Delta$ (in our example $1. < w_{\rm F}\Delta < 1.14$), this increase of pairing correlations versus T (near $T = 0$) can even generate a *reentrance phenomenon* with two transition temperatures (Fig. 1-b). In such a case pairing is absent at $T = 0$; as T increases, it switches on at some low critical temperature, then switches off at the higher familiar critical temperature [8,11]. The two critical temperatures merge for $w_{\rm F}\Delta \approx 1$, which corresponds to $w_{\rm F}\tilde{G} \approx 0.225$; for weaker values there exists no superconductivity in odd systems, whatever the temperature. In contrast, in even systems, pairing does not disappear until $w_{\rm F}\tilde{G} < 0.182$.

The comparison of (a) and (b) in Fig.2 shows that, at all temperatures, the even-N gap resists magnetic fields better than the BCS gap. It is also seen on Fig.2 that, at $T = 0$, the gaps $\Delta_{\rm F}$ do not depend on the magnetic fields; this is because the field intensities are such that $B < \Delta$. When $B > \Delta$, for the value $w_{\rm F}\Delta \approx 1.19$ of Fig. 2, pair correlations disappear completely. By comparing (b) and (c) one sees that the odd-N gap is significantly smaller than its BCS counterpart and more easily distroyed by the paramagnetic effects. Nevertheless, the growth with T of the odd-N gap at small T persists in the presence of a sufficiently small magnetic field.

Once the self-consistent equations (4) and (6) are solved, the *projected* average particle number, magnetization, energy, entropy (and hence the other thermodynamic quantities) can be obtained from the formulae

$$\begin{aligned}
\langle\hat{N}\rangle &= \sum_p \Big[1 - \frac{\epsilon_p - \mu}{\tilde{e}_p}(t_p + t_{\bar{p}})\frac{1 + \eta r_0 (t_p t_{\bar{p}})^{-1}}{2(1 + \eta r_0)}\Big] \quad , \\
\langle\hat{M}\rangle &= \sum_p (t_p - t_{\bar{p}})\frac{1 - \eta r_0 (t_p t_{\bar{p}})^{-1}}{2(1 + \eta r_0)} \quad , \\
\langle\hat{H}\rangle &= \sum_p \Big[\epsilon_p - \frac{\epsilon_p(\epsilon_p - \mu) + \frac{1}{2}{\Delta_p}^2}{\tilde{e}_p}\times \\
&\qquad (t_p + t_{\bar{p}})\frac{1 + \eta r_0 (t_p t_{\bar{p}})^{-1}}{2(1 + \eta r_0)}\Big] - B\,\langle\hat{M}\rangle \ , \\
S &= S_{\rm BCS} - \frac{\beta\eta r_0}{2(1 + \eta r_0)}\sum_p [(t_p^{-1} - t_p)e_p + p \leftrightarrow \bar{p}] \\
&\qquad + \ln[\tfrac{1}{2}(1 + \eta r_0)] \quad .
\end{aligned}$$

These quantities satisfy the fundamental thermodynamic relations, as warranted on general grounds by the variational nature of our approximation. Various limits (low and high temperatures, continuous level density, large volume) and numerical illustrations are worked out in [8] for $B = 0$, showing the qualitative differences between even and odd systems in physical quantities such as the specific heat.

Here we show on Fig.3, for the same values of $w_{\rm F}\Delta$ and of the magnetic fields as in Fig. 2, the magnetization $\langle\hat{M}\rangle$ versus the ratio T/T_c for the BCS theory, for the even ($N = 100$) and for the odd ($N = 101$) projected cases. All the curves converge to the Pauli paramagnetic values $2w_{\rm F}B$ at high enough temperatures. Until the B-dependent transition temperature is reached, the BCS magnetization is always larger than the even-N one, but both behave similarly. The behavior at small T of the odd-N curves is markedly different. While for $B = 0$ the magnetization is zero as expected, any value of B, however small, lifts the single-particle degeneracy of the spectrum and causes the zero-temperature value of $\langle\hat{M}\rangle$ to take integer values. For the small magnetic fields considered here ($w_{\rm F}B < 1$), one has $\langle\hat{M}\rangle = 1$ for $T = 0$. As T grows, $\langle\hat{M}\rangle$ increases or decreases in odd systems, depending on the value of B, so as to reach eventually

the Pauli paramagnetic value.

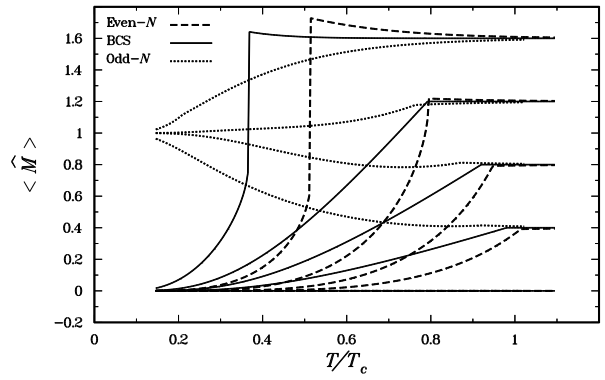


FIG. 3. The magnetization $\langle\hat{M}\rangle$ versus T/T_c for different values of the magnetic field B and for $w_{\rm F}\Delta = 1.19$ ($w_{\rm F}\tilde{G} = 0.233$). The dashed lines correspond to the even-N projection ($\langle\hat{N}\rangle = 100$), the solid lines to BCS ($\langle\hat{N}\rangle = 100$) and the dotted lines to the odd-N projection ($\langle\hat{N}\rangle = 101$).

Our curves exhibit a spurious non-analytic behavior at the critical points. This is a consequence of the approximation (2) which, like the BCS one, gives rise to either a broken or an unbroken invariance with respect to $\hat{N}$, depending on the temperature. In the exact treatment of a finite system without sources, the order parameter should always be zero and there can be no discontinuity at any temperature. However, allowing an order parameter while restoring the broken symmetry may reproduce the rounding-off of the transition [12]. For instance, in the present problem the difficulty above may be removed by replacing $\hat{P}_\eta$ by the projection $\hat{P}_{N_0} = (2\pi)^{-1}\int_0^{2\pi} {\rm d}\theta\, \exp(i\theta[\hat{N} - N_0])$ on the particle number N_0, thus restoring the invariance broken by $\hat{W}$. However, in this case the trial Ansatz $\hat{\mathcal{D}}(\tau) = \hat{P}_{N_0}\hat{T}(\tau)\hat{P}_{N_0}$, where $\hat{T}(\tau)$ is the exponential of the most general quadratic form in $a_i^\dagger$ and a_j, must include projections on both sides [8]. (In contrast, the Ansatz (2) contains a single projection since $\hat{P}_\eta$ commutes with $\hat{W}$.) After the substitution of $\hat{P}_\eta$ by $\hat{P}_{N_0}$, which amounts to replacing a two-term sum by a double integral over θ, the functional (1) remains an operational tool since one can still use Wick's theorem. The optimization of (1) then provides a generalization of the HFB theory which takes properly into account the particle number. In this scheme, where variation is performed after projection, the quantities $u_p\, v_p$ are expected to be non-zero at any temperature, and to yield smooth transitions. Likewise, in (cold) deformed nuclei the evolution of the moment of inertia with respect to the angular momentum is smoothened by the $\hat{P}_{N_0}$-projection, in agreement with the data [13].

Projected fluctuations and correlations could be evaluated, along the lines of Sect.4 of [8], through the expansion of $\varphi(\xi)$, as given by (1), up to second order in the sources ξ_γ. Finally, as proposed in [14], transport properties could be worked out by combining the static variational principle (1) with a time-dependent one.

One of us (M.V.) gratefully acknowledges the support of the Alexander von Humbolt-Stiftung and the hospitality of the Physics Department of the Technische Universität München.

[1] A.Bohr and B.R.Mottelson, *Nuclear Structure*, Vol.II (W.A. Benjamin, 1975).

[2] M.T.Tuominen, J.M.Hergenrother, T.S.Tighe, and M.Tinkham, Phys. Rev. Lett. **69**, 1997 (1992); P.Lafarge, P.Joyez, D.Esteve, C.Urbina, and M.H.Devoret, Phys. Rev. Lett. **70**, 994 (1993).

[3] D.C.Ralph, C.T.Black, and M.Tinkham, Phys. Rev. Lett. **74**, 3241 (1995); **76**, 688 (1996); **78**, 4087 (1997).

[4] P.Ring and P.Schuck, *The Nuclear Many-Body Problem* (Springer-Verlag, New-York/Berlin, 1980).

[5] D.V.Averin and Yu.V.Nazarov, Phys. Rev. Lett. **69**, 1993 (1992); B.Jankó, A.Smith, and V.Ambegaokar, Phys. Rev. B **50**, 1152 (1994); D.S.Golubev and A.D.Zaikin, Phys. Lett. A **195**, 380 (1994); R.A.Smith and D.V.Ambegaokar, Phys. Rev. Lett. **77**, 4962 (1996); K.A.Matveev and A.I.Larkin, Phys.Rev. Lett. **78**, 3749 (1997).

[6] J. von Delft, A.D.Zaikin, D.S.Golubev, and W.Tichy, Phys. Rev. Lett. **77**, 3189 (1996).

[7] F.Braun, J. von Delft, D.C.Ralph, and M.Tinkham, Phys. Rev. Lett. **79**, 921 (1997).

[8] R.Balian, H. Flocard, and M. Véneroni, Extended BCS Theories, nuc-th/9706041.

[9] E.Gerjuoy, A.R.P.Rau, and L.Spruch, Rev. Mod. Phys. **55**, 725 (1983); R.Balian and M. Véneroni, Ann. Phys. (*N.Y.*) **187**,29 (1988).

[10] R.Balian and E.Brézin, Nuovo Cimento **B 64**, 37 (1969).

[11] The reentrance effect can be inferred from the Fig.1-a of Ref. [6] by imagining cuts of the (implicit) surface of this figure by planes perpendicular to the $d/\tilde{\Delta}$ axis for values slightly larger than 0.89, which corresponds to $w_{\rm F}\Delta = 1.15$ on our Fig. 1-b.

[12] B. Mühlschlegel, D.J. Scalapino, and R. Denton, Phys.Rev. **B6**, 1767 (1972).

[13] See for instance, B. Gall, H. Flocard, P. Bonche, J. Dobaczewski, and P.H. Heenen, Zeit.Phys. **A348**, 89 (1994).

[14] R.Balian and M. Véneroni, Nucl.Phys. **B408** [FS], 445 (1993).